THE 1928 PLOVDIV SEQUENCE: FAULT MODEL CONSTRAINED FROM GEODETIC DATA AND SURFACE BREAKS

Dimitar Dimitrov[1], Jean-Claud Ruegg[2], Bertrand Meyer[3,4], Jean-Bernard Chabalier[2], Emil Botev[1], Pierre Briole[5]

[1]National Institut of Geophysics, Geodesy and Geography, BAS, e-mail <clgdimi@abv.bg>.
[2]Institut de Physique du Globe, CNRS UMR 7154, Paris, France.
[3]UPMC Univ. Paris 06, ISTEP, UMR 7193, F-75005, Paris, France.
[4]CNRS, ISTEP, UMR 7193; F-75005, Paris, France.
[5]École normale supérieure, F-75230, Paris, France.

Key words: *sequence of earthquakes, geodetic data, fault model, North Aegean*

Abstract: *Two destructive earthquakes (M=6.8 and M=7.0) occurred on April 14 and April 18, 1928, near the city of Plovdiv, in Southern Bulgaria. These are among the largest earthquakes that occurred in Europe and the Eastern Mediterranean area during the 20th century. A detailed analysis of the tectonic observations available in the literature allows us to determine that the 1928 sequence reactivated successively two antithetic faults of respectively 38 and 53 km length within the Maritsa Valley. The displacement is mainly normal and consistent with the available seismological data. We use an exceptional geodetic data set, formed by 500 km of levelling lines and GPS measurements of a former triangulation network to characterise the co-seismic displacement field. The deformation is asymmetric and mostly related to the second shock on a north-dipping fault with a maximum vertical displacement of 2 m. We reproduce this displacement field and the surface breaks using a model of dislocation in homogeneous elastic half-space. The model requires a south-dipping faulting north of the Maritsa with uniform slip of 0.7 m during the first shock. The second shock accounts for 75% of the seismic moment of the sequence and corresponds to the activation of a north-dipping fault cutting obliquely across the Maritsa Valley. Fault dip appears steeper near the surface and the maximum slip amounts to 2.6 m. These earthquakes occurred on faults located within the Maritsa depression and did not reactivate the large faults located by the edge of neighbouring reliefs.*

ЗЕМЕТРЕСЕНИЯТА ОТ ЧИРПАН – ПЛОВДИВ 1928 Г. – ГЛАВНИ РАЗЛОМИ ОТ ГЕОДЕЗИЧЕСКИ ДАННИ И ТЕРЕННИТЕ РАЗКЪСВАНИЯ

Димитър Димитров[1], Жан-Клод Руег [2], Бертранд Мейер [3,4], Жан-Бернар Шебалие [2], Емил Ботев[1], Пиер Бриол [5]

[1]Национален институт по геофизика, геодезия и география, БАН, e-mail <clgdimi@abv.bg>.
[2]Institut de Physique du Globe, CNRS UMR 7154, Paris, France.
[3]UPMC Univ. Paris 06, ISTEP, UMR 7193, F-75005, Paris, France.
[4]CNRS, ISTEP, UMR 7193; F-75005, Paris, France.
[5]École normale supérieure, F-75230, Paris, France.

Резюме: *Двете катастрофални заметресения от 14 и 18 Април 1928 г. в районите на Чирпан и Пловдив с M=6.8 и M=7.0 са от най-силните в Европа и източното средиземноморие през 20 век. Детайлният анализ на тектонските изяви определят, че двете земетресения са реактивипали два антитетични разлома с дължина респективна 38 и 53 кт по Маришката долина. Ние използваме изключителните геодезически данни от 500 km повторни нивелачни измервания и данни от преизмерената с GPS триангулачна мрежа за да характеризираме полето на ко-сеизмичните премествания. Възстановихме тези премествания и терените деформации, използвайки дислокационен модел за хомагенна еластична полусреда. Моделиранео показва, че един нармален разлом (разсед) с наклон на юг и хлъзгане от 0.7 m е свързан с първият трус от 14 Април 1928 г. Вторият трус освобождава 75% от сеизмичния момент на двата труса и е свързан с активирането на разсед пропадащ на север и пресичащ Маришката долина. Този разлом променя наклона си в дълбочина и има максимално хлъзгане от 2.6 m. Двете земетресения от Април 1928 г. са станали в Маришката депресия и не са активирали големите разломи определящи релефа от двете страни на Горнотракийската низина.*

Introduction

On April 14 and April 18, 1928, two major earthquakes struck southern Bulgaria near the city of Plovdiv [1]. The epicentres were located along the Maritsa valley between the Rhodope and the Balkan Mountain belts. This sequence was among the largest recorded in the Eastern Mediterranean region during the 20th century [2] with estimated magnitudes of 6.8 and 7.0 respectively [2, 3 4]. Fifteen aftershocks with magnitude M>5 were recorded during the following month. The two main shocks and the subsequent aftershocks hit a large area of about 3000 km^2 and caused important damage including the destruction of 5 towns and more than 240 villages.

The fault parameters of the sequence are estimated using mainly two kinds of documents: contemporary reports describing the effects of the events [5, 6, 7, 8, 9, 10] and a comparison of levelling data acquired before and after the earthquake and some of which has been published by [11, 12. 13]. Up to 506 km of levelling lines have been surveyed by the National Cartographic Institute of Bulgaria (NCI) before and after the events. Mirkov [11] presented the results of the co-seismic elevation changes in cross sections along selected profiles. Yankov [12, 13] provided a map of co-seismic displacement by interpolating the data published by [11] and proposed an interpretation. From contemporary observations and/or subsequent levelling measurements, several determinations of the source parameters have been proposed [1, 14, 15]. More recently a quantitative model has been proposed by [16] on the basis of the levelling data alone. All those interpretations relate the first event to two antithetic faults within the Maritsa river banks and the second event to a single fault cutting further west across the river.

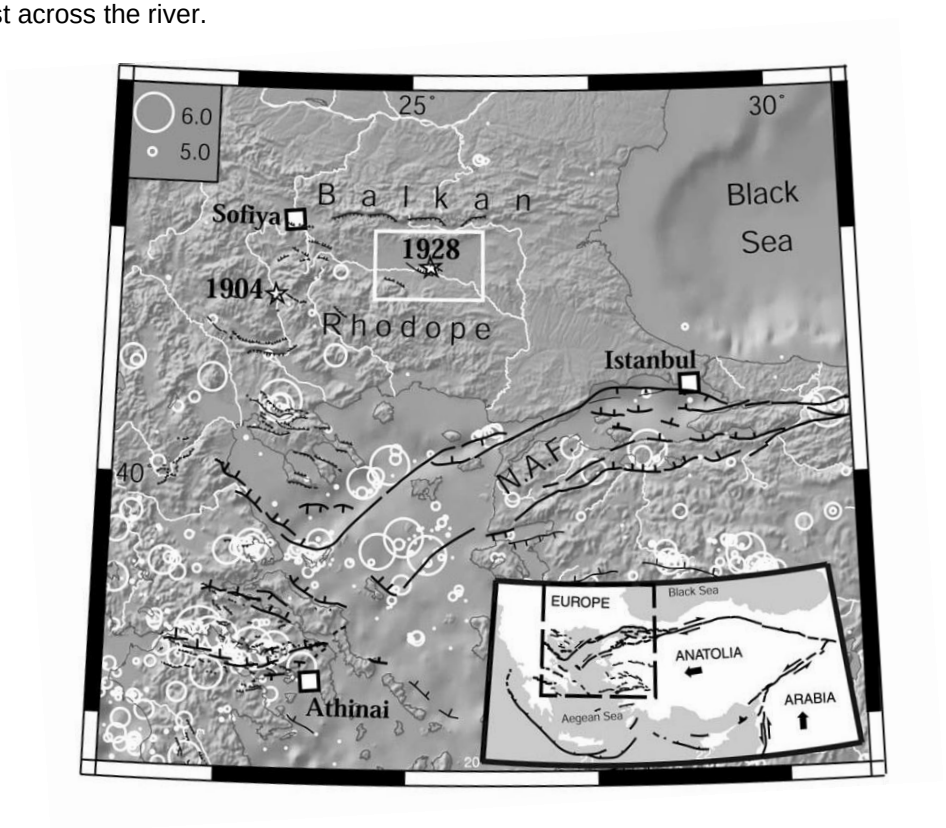

Fig. 1. Seismotectonics of the North-East of the Mediterranean area. Seismicity (1964–1999) from the ISC catalogue. White stars indicate location of the 1904 Struma and 1928 Plovdiv earthquakes. NAF. relates to the North Anatolian Fault system termination in the Aegean. Active faults compiled from bathymetry, geological studies and satellite imagery by [19, 20, 23]. White box outlines the Plovdiv area enlarged in the following figures.

We revised the available data associated with this sequence to refine a quantitative deformation model. All the documents describing the field effects have been reanalysed and combined with available seismological data, to discriminate between the main surface ruptures of the two events and secondary effects. The original field archives of the levelling data [11] and two other unpublished levelling lines, measured in 1940 and 1959 have been re-adjusted using a new compensation process. The data provides an exceptional set of co-seismic elevation displacements of 349 benchmarks that intersects the fault breaks at 8 points. A former triangulation network installed in 1926 and measured with GPS in 1993 provides estimates of the co-seismic horizontal displacements [16] and is also used to derive a refined fault model. Finally we discuss this model with the large-scale tectonic implications in relation to the nearby extension in the North Aegean region.

Regional Tectonics and Active Faulting

The earthquakes of April 14 and April 18, 1928 occurred north of the Aegean Sea in the upper Thrace lowland of Bulgaria (high Maritsa valley) between the Rhodope range to the South and the crystalline Balkan Mountain to the North (Fig. 1). The structural trend is almost NS in the Dinarides and the Hellenides in the East turns NW-SE in the Rhodope to EW in the Balkan, as outlined by the topography and the large river courses (Fig. 1). These belts have been formed mainly in the late Mesozoic and the early Tertiary as crustal shortening took place between the converging Africa and Eurasia plates After the Oligocene, the region has experienced mostly NS crustal extension and is considered to be the northernmost part of the stretched Aegean domain [14]. The driving mechanism of this extension remains controversial. Some authors have proposed high stretching rates with crustal thinning during the last 5 Ma [14] or during a poly-phased evolution, during the last 25 Ma [17, 18]. Another view has proposed a two stage evolution resulting from the recent propagation of the North Anatolian fault into the already slowly extending Aegean domain [19, 20]. In Bulgaria, the normal faults strike mostly EW to ESE and are slightly oblique to the fabric in the Rhodope and the Balkan belts. These faults are less developed than in central Greece and western Turkey (Fig. 1), where some of them have ruptured during destructive earthquakes with clear surface breaks: Thessaloniki, Ms=6.4 in 1978 [21, 22] and Grevena Ms=6.6 in 1995 [23]. In Bulgaria, the sequence of two destructive earthquakes separated by 23 minutes that occurred in 1904 in the Struma valley, west of the Rhodope (Fig. 1) resembles the 1928 Plovdiv sequence [23]. The 1928 sequence occurred along EW asymmetric graben of the high Maritsa valley floored by Neogene and Quaternary alluvial sediments. The sequence is usually assigned to relatively minor normal faults inside the graben compared to the large faults located on both sides of the valley. A conspicuous normal fault, the Asenovgrad fault, marks the southern edge of the graben at the edge of the Rhodope massif and lies close to the epicentre area. Neither its seismic potential nor its current activity has been well assessed although ten destructive earthquakes (I>VIII) are reported in the area during the last millennium [2, 24].

Observations of Surface Breaks and Seismological Constrains

Important surface effects are associated with the 1928 sequence. Breaks of 105 km total length, producing a large subsiding area in the Maritsa valley, with the formation of several temporary lakes and landslides have been reported. The descriptions, maps and reports of tectonic observations were made soon after the earthquake sequence [5, 6, 7, 8]. The most detailed descriptions of surface ruptures, including many photographs have been published by the National Commission for the mitigation of seismic damage [9] and in two monographs published by the Bulgarian Academy of Science[25, 26]. The simplified rupture map published by [5] is considered by the scientific community as the basis of the fault parameters determination for this sequence. For the first shock, the authors identify two antithetic fault ruptures, one north of Chirpan, dipping south, the other one south of Chirpan, dipping north. For the second shock they map another rupture, 20 km to the west on a single fault that cuts the river (Fig. 2). The higher Intensity contour (I=X) of the isoseismic map published by [5, 9] is shown in Figure 2. The effects of the two separate shocks can be clearly identified using the military reports performed immediately after the first shock and the subsequent reports following the second shock: the isoseismal map of the shock from April 14 is centred on the city of Chirpan whereas that of April 18 centres 20 km to the West, near to the city of Belozem.

We have reconsidered all the available data in order to distinguish the main surface breaks from secondary effects for each of the main shocks. In the following section we discuss the surface observations together with the available seismological data and the geomorphology.

The April 14 event activated two zones: A badly damaged area, located to the north of Chirpan, clearly associated with the 38 km continuous rupture between Trakia and Orizovo, striking N95° and dipping to the south. Continuous normal scarps with an average of 40 cm down-to-the-south slip (reaching a maximum of 50 cm in the middle of the rupture NW of Chirpan) were measured [9]. The settlements situated along the mapped rupture - Chirpan, Tcherna Gora, Orizovo, Partizanin, Gorno Belovo, Svoboda – were totally destroyed [9]. This leaves the doubt that this 38 km continuous rupture is associated with a fault activated during the first shock. This rupture outlines the base of a small topographic relief of 10 to 20 m, which corresponds to cumulative slip of on the Chirpan fault [27]. The evidence of en echelon fissures and a few centimetres of horizontal offsets of the roads indicate a limited right lateral component of slip [9].

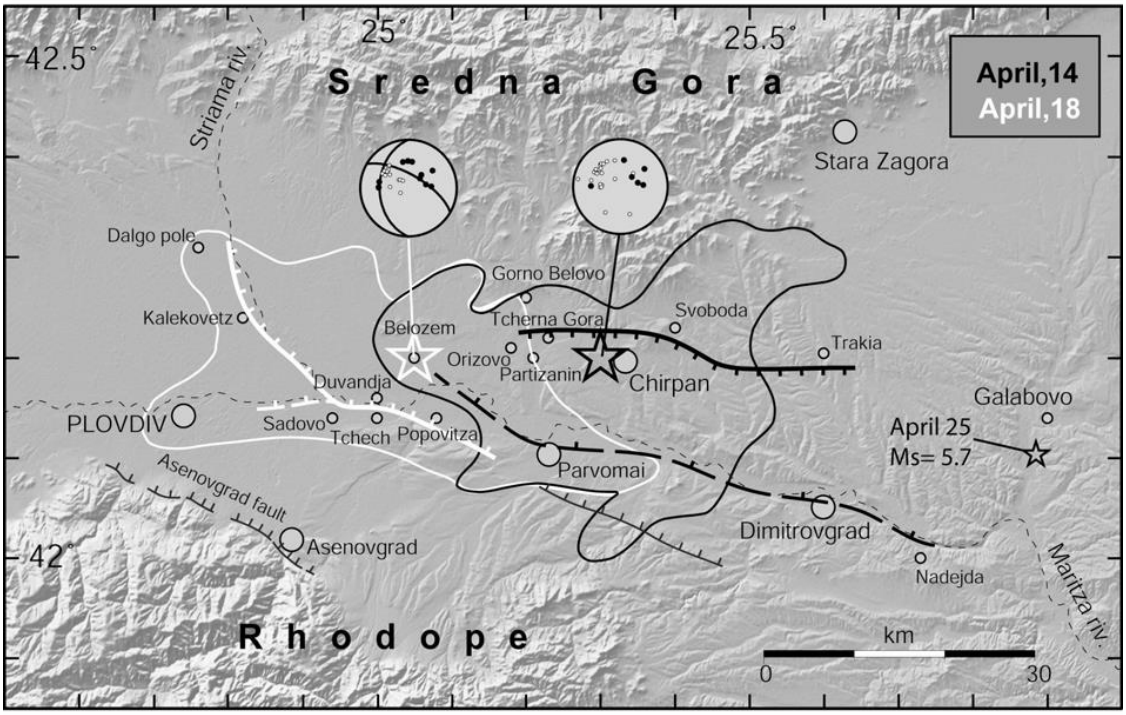

Fig. 2. Field effects of the Plovdiv, 1928 sequence [5]. Black symbols relate to the 14 April shock, and white symbols to the 18 April shock. Thin lines correspond to areas that have been destroyed by the 1928 sequence (Intensity > X). Black and white stars indicate epicentre estimation of each shock from instrumental and macro-seismicity (see text and Table 1 for details). Thick lines relate to clearly identified ruptures of each event and dashed lines to secondary effects observed along the Marisa River. Ticked thin lines correspond to recognized normal faults. First motion arrivals are plotted on a lower hemisphere for each event allowing the focal mechanism of the second shock to be determined.

Another area 12–15 km to the south of the main rupture experienced significant ground shaking during the April 14 event. Discontinuous surface breaks have been described along the southern bank of Maritsa River between the cities of Nadejda and Belozem]5, 9]. They consist mainly of fissures and small steps with up to 20 cm down-to-the-north offsets. Many impressive ground surface manifestations in this area have been reported: landslides near the Maritsa River, craters, flooded zones. A huge vertical offset of 3.5 m probably associated with a restricted landslide, has been locally reported by [7]. The village of Liubenovo (now Parvomai) was flooded by more than 70 cm of water. Nonetheless the destruction was much less than north of the river and the few villages on the southern shore were not significantly damaged by the first shock, e.g. Debar located 3 km South of Parvomai, Popovitza and Tchechnigirovo [9]. These observations suggest that the southern area was mainly affected by superficial effects of non tectonic origin such as slumping and landsliding. This is also a conclusion of the palaeoseismic studies conducted in the epicentre region by [27].

Table 1. Seismological parameters of the Plovdiv earthquakes of April, 1928

	April 14, 09:00:46 TU:						
No	φ (°)	λ (°)	h (km)	M	Io	determination	references
A1	42.2° N	25.33° E	15-20	-	X	macros	Kirov & Grigorova, 1961
A2	42.21° N	25.36° E	10	6.8	-	instrum	Christoskov & Grig., 1968
A3	42.2° N	25.3 ° E	7	6.8	X	macros	Karnik, 1969
A4	42.2° N	25.3 ° E	9	6.8	IX	macros	UNESCO, 1974
A5	42.13° N	25.28° E	-	-	X	macros	Christoskov & Grig., 1968
A6	41.7 ° N	26.3 ° E	-	6.8	-	instrum. ISS	Karnik,1969
	April 18, 19:24:04 TU :						
B1	42.17° N	25.05°E	20-25	-	XI	macros	Kirov & Grigorova, 1961
B2	42.2° N	25.05°E	16	7.0	IX-X	macros	UNESCO, 1974
B3	42.13° N	25.02°E	-	-	XI	macros	Christoskov & Grig., 1968
B4	42.12° N	25.07°E	7	7.1	-	instrum.	Christoskov & Grig., 1968
B5	42.1° N	25.0° E	10	7.0	XI	macros	Karnik, 1969
B6	41.8° N	25.0° E	-	6.3/4	X	instrum. ISS	Karnik, 1969

Table 1 lists the six available epicentre estimations of the first shock. With the exception of the instrumental determination A6 which is located 100 km away from the others, all fall close to the reported ruptures. The determinations from A1 to A4 are concentrated in a small area (less than 10 km square) centred to the town of Chirpan. We represent the barycentre of the solutions A1-5 (42.18°N; 25.32°E) in Fig. 2 and assume it corresponds to the plausible epicentre of the first shock. The hypocenter of this event is located at approximately 10 km depth. No seismological determination of the fault plane solution has been proposed for the first shock. The one given by [14] relies on the reported surface breaks. To further estimate the focal mechanism of this event, we collected the available data of P first arrivals from the European seismic stations. The positions of “dilatation” and “compression” are consistent with normal faulting (Table 2).

Table 2. The focal mechanisms determination of the Plovdiv earthquakes of April, 1928

No	determination from		strike(°)	dip(°)	rake(°)	note
	April 14, 1928 :					
(a)	Jackson & McKenzie,1988		105°	45°	-90°	Ms=6.9
	April 18, 1928 :					
(a)	Glavcheva,1984 (upper semi-sphere)		105°	79°	-	(Figure in paper)
(b)	Jackson & McKenzie,1988		125°	45°	- 90°	Ms=6.9
(c)	Dimitrov & Ruegg,1994		305°	67°	-	(Figure in paper)
(d)	Van Eck & Stoyanov,1996	- plane A:	97°	57°	-	
		plane B:	191°	79°	-	
(e)	This study	- plane A:	180°	40°	- 37°	
		plane B:	300°	67°	- 123°	

New surface ruptures were associated with the second shock of April, 18. A 53 km long main rupture with clear scarps down-to the North was observed [9]. It started 10 km SW of Parvomai and extended parallel to the scarp of the Rhodope massif in a direction approximately N118°E. It crossed Maritsa River between Popovitza and Duvandja forming a waterfall 1.5 m high, then followed the Striama River farther NW, with a direction N 144°E, and ended near the village of Dalgo Pole, 20 km north of Plovdiv. Another 10 km rupture along Maritsa River was mapped. It was connected with the main rupture at the confluence with the Striama River (Fig. 2). The most important displacements have been observed in the eastern part of the rupture from April, 18. A vertical displacement of 1.5 m was observed SW of Popovitza village [5]. It coincides with a significant 30-40 m topographic scarp that can be followed up to Parvomai, corresponding to a minor pre-existing normal fault. However, no cumulative fault scarps are associated with the NW extension of this rupture along Striama River - N118°E. Moreover, in the Maritsa basin many complex secondary fissures and ruptures quasi-parallel to the main rupture have been mentioned by different authors. Between the villages of Popovitza and Duvandja a vertical offset of about 3 m has been reported. The villages situated between Parvomai and Sodovo were flooded [25]. Evidence of right-lateral components of slip is shown by the analysis of 62 photographs: in echelon fissures, bayonet features, deformed railway, chimney and monuments [9, 27]. In conclusion the April, 18 shock activated unequivocally a 53 km normal fault dipping NE that will be named “Popovitza fault” hereafter.

Soon after the two earthquakes different authors mentioned the flow variations of 350 mineral springs, a phenomenon, frequently observed for normal faulting, that can be associated with the co-seismic strain changes [29]. The strongest aftershock of M=5.7 occurred on April 25 near the city of Galabovo [30], but no particular surface ruptures have been reported (Fig. 2).

Six estimations of the epicentre location have been proposed by different authors (Table 1). Except B6 located in the Rhodope Mountains all epicentre locations are concentrated around Popovitza village where the maximum vertical offset was observed. We consider only B1 and B2 solutions located north of the rupture at epicentre (42.18°N, 25.05°E, white star on Figure 2). The hypocenter of this shock seems to be deeper than the April 14 shock (~15 km). Two slightly different focal mechanisms of the April 18 shock have been proposed by [31, 32]. Dimitrov & Ruegg [16] calculated a solution close to that of Glavcheva (1984). We collected new data from European stations (27 additional first arrivals) and determined a reliable focal mechanism presented in Figure 2 (strike=300°, dip=67°, rake=-123°). The plane dipping to the North fits well with the azimuth of the main surface rupture. The small right lateral component of slip is consistent with the field evidence.

The 1928 Plovdiv sequence reveals the reactivation of two antithetic normal faults – the

"Chirpan fault" and the "Popovitza fault" - that correspond to minor pre-existing faults. No rupture was observed along the Asenovgrad fault, 10 km to the south of Plovdiv that shows clear morphological evidence for young Quaternary slip with a topographic scarp greater than 1000 m (Fig. 2) and appears to be geologically the most active fault in the region.

Geodetic data

The National Cartographic Institute of Bulgaria (NCI) installed the National levelling network in the Plovdiv region from 1923 to 1927 (Fig. 3). The levelling surveys were performed by classical 1st and 2nd order method of double run, using spirit levels and invar rods. After the seismic sequence of April, 1928, 506 km of levelling lines were re-measured by NCI in 1929–1930 using the same methodology and instruments. The random error for these surveys is estimated at ±1.5 mm/km. After adjustment of the two epoch data [11] estimated the co-seismic elevation changes with accuracy better than 1 cm. Mirkov [11] analysed the 1923–1927 and 1929–1930 levelling data and presented the map of levelling network and selected profiles of the co-seismic changes. Yankov [12, 13] cited by [1], published a map of co-seismic changes with isolignes deduced from the levelling data published by [11].

Using the same data set from [12, 13, 16] proposed a model of co-seismic deformation. Now we model the same data set, adding the Nova Zagora - Maritsa levelling line re-measured in 1940 and the Plovdiv-Karlovo levelling line re-measured in 1959 (Fig. 3). Finally, we re-adjusted the position of all the available data together in order to determine the co-seismic elevation changes of 349 levelling benchmarks Fig. 3 presents the position of the benchmarks used in this study and Fig. 4 the selected profiles. It is worth noticing that this extensive levelling data set cumulates the co-seismic displacement fields of the April 14 and April 18 shocks without allowing for distinguishing their respective effects.

The levelling data show 8 points A, B, C, D, E, F, G and H (Fig. 3 and Table 3) where the surface vertical co-seismic breaks are directly evaluated and are in very good agreement with the map of the main ruptures (Fig. 3) and their descriptions in the previous section.

In the area affected by the April, 14 shock (Fig. 2) a 15 km wide asymmetric zone of subsidence with a maximum down-throw of 46 cm, is observed between Maritsa River and Chirpan fault (Fig. 3 and Fig. 4, profiles e-e'). An uplift zone with a maximum displacement of 24 cm (Table 3) is observed to the north of the Chirpan fault (Fig. 3 and Fig. 4, profiles e-e' and f-f'). The small displacements in the southern part of the area (Fig. 3 and Fig. 4, profiles e-e' and f-f') and these on the Parvomai - Dimitrovgrad levelling line show that the observed field effects along the Maritsa River cannot be associated with fault slip.

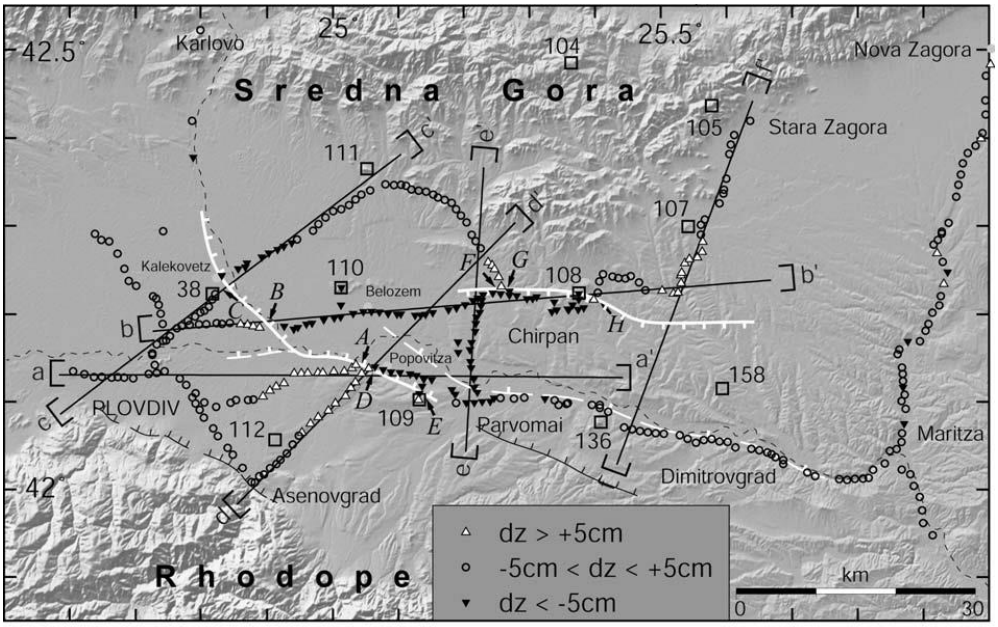

Fig. 3. Location of the geodetic data used in this study. Displacements of levelling benchmarks are plotted according to their elevation changes. Open circles correspond to small elevation changes < 5 cm, white triangles to uplift > 5 cm and reverse black triangles to subsidence > 5 cm. Capital letters A, B, C, D, E, F, G and H correspond to intersections of the levelling lines with the fault breaks, where direct measurement of vertical offsets has been done (Table 3). Profiles a-a' to f-f' refer to the cross sections presented on Fig. 4. Open squares corresponds to triangulation pillars measured in 1926 and re-measured by GPS in 1993 [16].

Table 3. Vertical offset at the intersection between the levelling lines and the rupture traces, A1 = maximum uplift, A2 = maximum subsidence, R = A1 / A2

Village	Point of Figure 4a	A1 (m)	A2 (m)	A1+A2 (m)	R = A1/A2	Dip (°)
Popovitza West	A	0.53	- 0.97	1.50	0.55	70
Belozem	B	0.07	- 1.05	1.12	0.067	40
Kalekovetz	C	0.02	- 0.31	0.33	0.079	40
Popovitza South	D	0.45	- 0.97	1.42	0.46	60 - 80
Triangul. Point 109	E	0.13	- 0.28	0.41	0.46	60 - 80
Tcherna gora	F	0.09	- 0.40	0.49	0.23	40 - 60
Chirpan NE	G	0.02	- 0.14	0.16	0.14	35 - 55
Svoboda	H	0.10	-----	-----	-----	-----

In the area affected by the April 18 shock (Fig. 2) a large subsidence zone with a maximal down-throw of 103 cm near Belozem (Table 3, Fig. 3 and Fig. 4, profiles b-b') is observed. An uplift zone is also observed SW of the Popovitza village with maximum displacement of 53 cm (Table 3, Fig. 3 and Fig. 4, profiles a-a' and d-d'). These observations are in good agreement with the main surface rupture of April 18 described in the previous section.

The very small displacements measured on the far levelling lines where surface breaks were not reported (Maritsa - Nova Zagora to the east and Plovdiv – Karlovo to the west) gives good confidence of the levelling data. No surface displacement associated with the April 18 shock are observed on the Asenovgrad fault (Fig. 3 and Fig. 4, profiles c-c' and d-d'). Both surface break observations and levelling data indicate that the sequence of the Plovdiv 1928 earthquakes activated two main faults: "Chirpan fault" (during the first shock on April 14) and "Popovitza fault" (during the shock on April 18). These two antithetic faults are not face to face but shifted laterally. The deformation is asymmetric with major faulting of the Popovitza fault (maximum break of 1.5 m) and Chirpan fault (maximum break of 0.5 m).

The first and second order pillar triangulation network was established and measured in 1925-1926 by NCI. The random error for the angular observations was estimated better than 1.0 arc sec [11]. Only five triangulation points in this region were re-measured in 1958. The maximal angular change of about 11.13" for a distance of 11.5 km indicates deformation of the network with displacements of approximately 50 cm. By using the well preserved original monuments of the network, GPS measurements were carried out in order to determine horizontal co-seismic deformations. The Central Laboratory of Geodesy of Bulgarian Academy of Sciences carried out the survey in 1993 in collaboration with Institut de Physique du Globe de Paris and the Cartographic Military Institute of Bulgaria [16]. The 1993 GPS measurements being more accurate than the triangulation coordinates provided the possibility of determining the displacement vectors 1926-1993 using least-square adjustment of the original angular observations, taking as reference the 1993 GPS coordinates. The fixed points are located on Sredna Gora Mountain, far from the affected zone (point 104 in Fig. 3 and Fig. 5). The results of the adjustment are presented in Fig. 5. Despite the low accuracy of the former triangulation measurements, the displacement vectors are consistent with NS to NNE-SSW extension of the zone with maximum displacement of 83 ± 20 cm of point 109, between Popovitza and Parvomai.

Modelling

To model the co-seismic surface displacements we use a dislocation embedded in an elastic half space [32]. We proceed by trial and error, integrating the tectonic and seismologic constraints, increasing progressively the complexity of the model in order to fit closely the levelling and the GPS data.

We first define the strike and the length of two main dislocations using the ruptures and the levelling data. For Chirpan fault, the 3 points F, G and H (Fig. 3) where the levelling lines intersect the rupture allows determination the strike and length of the dislocation (respectively N 95°E and 36 km) in good agreement with the mapped rupture. For Popovitza dislocation we determine the strike of the plane by adjustment of the 5 aligned levelling points A, B, C, D and E (Fig. 3) which separate the hanging wall from the footwall (N 299°E). The length has been fixed to 31 km, according to the mapped rupture. This is consistent with the focal mechanism determined previously (N 300°E, Table 2).

Second we use these two single dislocations to determine the dip of the faults taking a rake fixed to 90° corresponding to a simple normal faulting. The subsidence/uplift Ratio (R) that can be

calculated at the points A, B, C, D, E, F, G and H (Fig. 3 and Table 3) is used to fix the mean dip at the different intersection points. The best fit of this ratio indicates the dips that vary from 40° to 70° (7th column of Table 3). For Chirpan fault, a dislocation with a dip of 60°, slip 70 cm and depth 10 km explains well the geodetic data with no greater complexity being required. For Popovitza fault: the best mean dip varies from one profile to another from 70° for points A, D, E to 40° for the points B and C (Table 3). Moreover no uniform dip model fits the hanging wall together with the footwall sides as well as the width of the subsiding area (i.e. on profile b-b', Fig. 4). The more important uplift of the footwall visible on profiles a-a' and d-d' (Fig. 4) indicates that the Popovitza fault has a steeper dip near the surface than at depth. Therefore a change of the dip with depth is required by the data in the model proposed by [16]. We consider 75° dip from the surface to a depth of 6.3 km and 45° to the total depth of 14 km. The variation of the vertical offset along this fault also requires some changes of the slip. Therefore we divide the dislocation in 5 sub-faults and invert the levelling data in order to determine the slip and the depth of all 10 resulting patches.

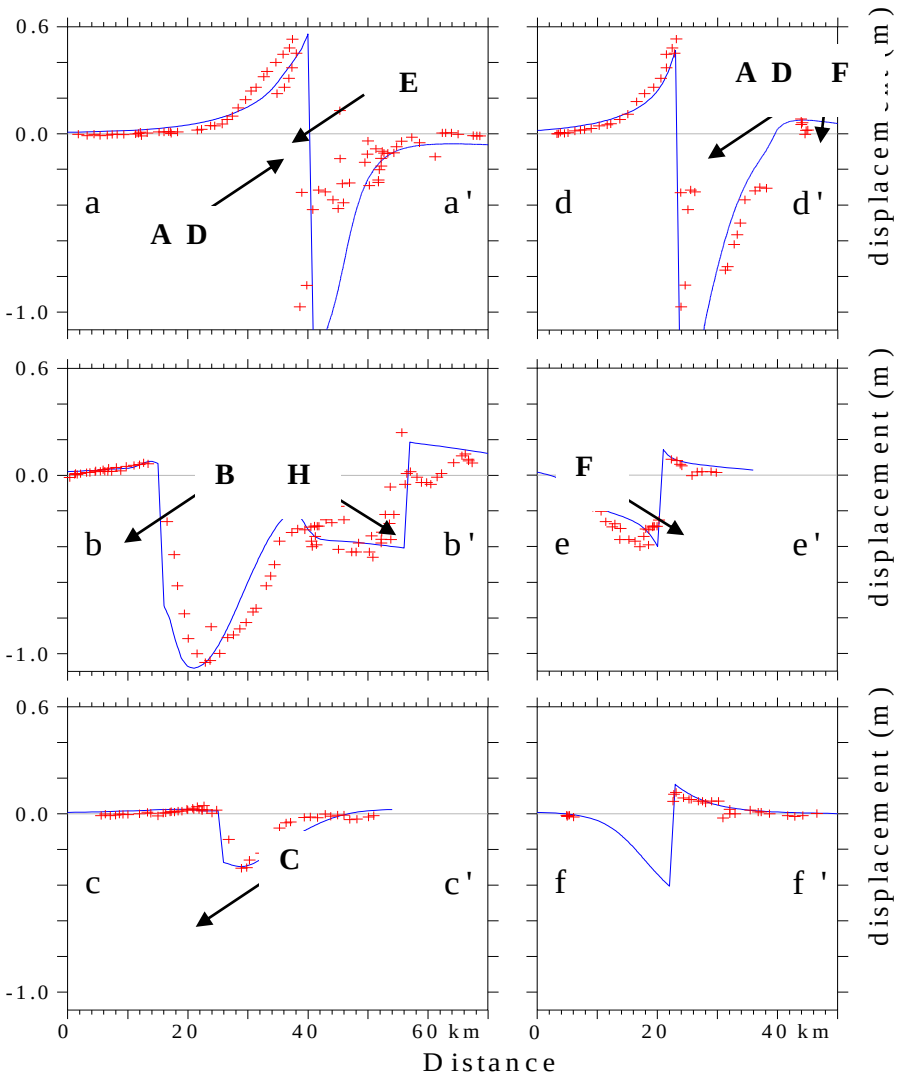

Fig. 4. Cross sections a-a' to f-f' (see location on Fig. 3) of the elevation changes from levelling are represented with crosses and modelled elevation changes by continuous lines. Slip distribution and geometry are presented on Fig. 5.

The final model consisting of 11 patches is shown in Fig. 5 and the corresponding parameters are given in Table 5. The comparison of the levelling data with the model is given in Fig. 4. The model explains well the amplitude of the vertical displacements and the width of the subsiding areas. The model reproduces accurately the uplift of the footwalls, as highlighted by the cross sections Fig. 4. Some misfit between measured and modelled displacements is nonetheless observed in the subsiding area and could be explained by secondary effects in the sedimentary basin. To explain the eastern extension of Chirpan fault, we maximize the length of the dislocation taking into account the observed surface rupture. The levelling data can explain a 10 km shorter dislocation towards the East that

reduces the seismic moment of this fault with 25%. The levelling data do not require any slip on the antithetic fault of April, 14 along the Maritsa River.

In Fig. 5 we plot the horizontal vectors resulting from the model. Except for the point 110, all the modelled vectors are inside the error ellipses, indicating good agreement with the measured vectors. We tried to improve the horizontal fit varying the rake of the slip vector with a right lateral component consistent with tectonic and seismological observations. A rake of 100°–120° does not improve the horizontal fit, and has no significant effect on the vertical displacement. These geodetic data are not able to resolve any lateral component of slip.

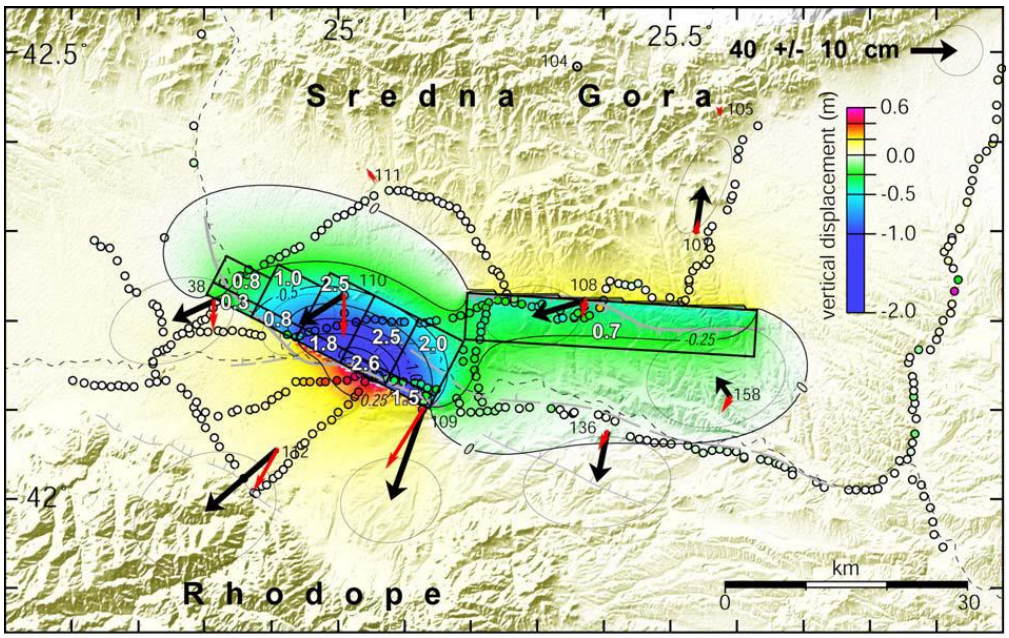

Fig. 5. Final model of 1928 Plovdiv sequence. Dislocations (black rectangles) with the corresponding slip (in meters, in white) that produce the vertical field displacement presented in colour with thin contour lines (every 0.25 m). The levelling data are represented with the circles coloured with the same convention as the model. The horizontal co-seismic vector observations with 95% confidence are plotted with black arrows and vectors predicted by the model with red arrows.

Table 5. Final dislocation model parameters: X, Y, h are UTM (WGS84, 35t) coordinates of the centre of the upper side of the fault (in km); φ and λ are the Azimuth and dipping angle of the fault element - in [°]; W and L - the width and length of each element in [km]; U is the normal slip - in [m]; M_o - the seismic moment in 10^{19} [Nm].

	X (km)	Y (km)	h (km)	φ (°)	λ (°)	W (km)	L (km)	U (m)	Mo x10[19] [N.m]
April 14, 1928 - one normal fault:									
	368.99	4675.59	0.0	94.5°	60°	11.55	36.0	0.7	0.96
Total moment:	$M_o = 0.96 \times 10^{19}$ [N.m],					$M_w = 6.7$			
April 18, 1928 - one listric complex fault composed by 10 following subfaults:									
1.	343.23	4664.24	0.0	298.58°	75°	6.57	6.2	1.5	0.201
2.	337.78	4667.21	0.0	298.58°	75°	6.57	6.2	2.6	0.349
3.	332.34	4670.18	0.0	298.58°	75°	6.57	6.2	1.8	0.242
4.	326.89	4673.14	0.0	298.58°	75°	6.57	6.2	0.8	0.107
5.	321.44	4676.11	0.0	298.58°	75°	6.57	6.2	0.3	0.040
6.	344.05	4665.73	6.3	298.58°	45°	10.83	6.2	2.0	0.443
7.	338.59	4668.70	6.3	298.58°	45°	10.83	6.2	2.5	0.554
8.	333.15	4671.67	6.3	298.58°	45°	10.83	6.2	2.5	0.554
9.	327.70	4674.64	6.3	298.58°	45°	8.00	6.2	1.0	0.163
10.	322.25	4677.60	6.3	298.58°	45°	5.17	6.2	0.8	0.106
Total moment:	$M_o = 2.77 \times 10^{19}$ [N.m],					$M_w = 7.0$			

Discussion and Conclusions

Our final model is consistent with the available seismologic and tectonic data. Taking a shear modulus of 33 GPa, it yields a seismic moment of 1.0 10^{19} Nm (M_w=6.7) for the April 14 earthquake and 2.8 10^{19} Nm (M_w=7.0) for the April 18 event (Table 5) consistent with the seismologic estimates (respectively M=6.8 and M=7.0).

For the April 14 shock the geodetic data can not resolve the eastern extension of the slip. Taking a 10 km shorter dislocation to the east leads to a moment of 0.7 x10^{19} Nm (M_w=6.6) slightly smaller than the above estimates. 73% of the total moment is released during the April, 18 shock on the Popovitza fault (Fig. 6). The antithetic Chirpan fault accommodates only 27% of the total moment corresponding to a slip of 70 cm. It could be interpreted as a consequence of the flexure of the hanging wall due to the major faulting observed along the southern system. The dominance of the southern system is observed during the 1928 sequence (Popovitza fault) as well as in the morphology (Asenovgrad fault, Fig. 2, Fig. 6).

The regional seismic activity recorded by the National Seimological Network between 1931 and 1980 in the Maritsa valley is moderate, with only 5 earthquakes of magnitude greater than 4 [33]. The uncertainties on the localisations do not allow any seismotectonic interpretation. The modern instrumental seismicity (M>2.5) from 1980 to 2003 is shown in Fig. 6. Most of the seismicity is located between 5 and 15 km depth, and exhibits two clusters. One is located around the April, 1928 ruptures. The second, located in the border of the Rhodope, occurred in 2002 and is probably associated to the Asenovgrad fault. Two events with M>4 have been localized, one in the Sredna Gora and the other near the April, 14 epicentre. No significant seismicity is observed north of the Maritza valley, where major active fault cuts longitudinally the Balkan belt (Fig. 1).

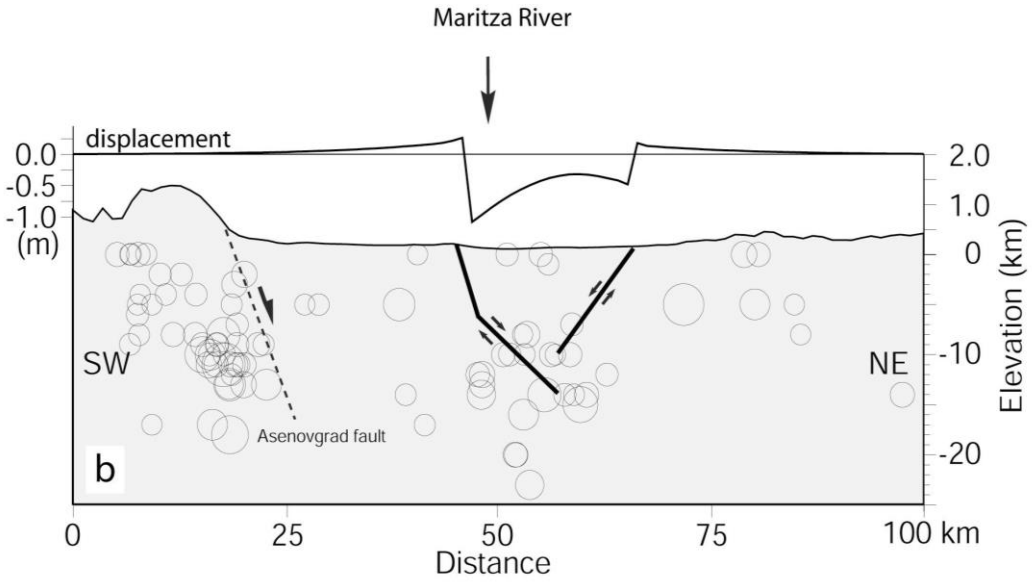

Fig. 6. Cross-section of the seismicity, fault model and topography projected from SW to NE. Note scale exaggeration for topography (x5 to the right). Top - surface vertical displacement predicted by model presented in Figure 5 (scale to the left).

The April 1928 sequence reactivated a normal fault system, formed by two antithetic faults of 36 and 62 km length with magnitudes of 6.8 and 7.0. Generally large normal faulting earthquakes (M>6) that struck the Aegean region and western Turkey during the last 30 years occurred on steep faults with a clear morphological signature recorded by the topography [23, 34]. Several authors also proposed that well-preserved escarpments around the eastern Mediterranean correspond to a signature of post-glacial faulting [20], where historical events occurred [35].

For the 1928 sequence, the cumulative topographies associated to the activated faults are small (20 m for the Chirpan fault and 0–40 m for the Popovitza fault), suggesting slow deformation rates. The Plovdiv sequence could have reactivated hidden old faults having low long term slip rate and infrequent earthquakes. This is compatible with the 0.15 mm/yr long-term slip-rate estimated for the Krupnik fault [23] that broke in 1904 in the South-west of Bulgaria and with its very long recurrence interval (greater than 14 ka [36].

The recent paleoseismic investigations of the antithetic Chirpan fault [27] identify at least three surface-rupturing earthquakes similar to the 1928 one, suggesting a Holocene rate of about

0.22 mm/yr, comparable to the one of Krupnik fault. A similar Holocene rate (0.2 mm/yr) has also been documented for the Kaparelli fault, an antithetic fault of the Corinth Rift. The penultimate event on the Kaparelli fault occurred 10 000 years before the 1981 earthquake sequence [36].

However, for the Chirpan fault, the recurrence interval estimated from the four last events is 2350 ± 643 years [27]. It is significantly less than the recurrence intervals for the Krupnik or the Kaparelli faults. For the Chirpan fault, the slip amplitude of the four late events is rather uniform, with an average of 0.51±0.05 m [27]) and 0.45 m observed during the 1928 earthquake. If we extrapolate these observations to the Popovitza fault and assume that the system has been activated during each event with a slip similar to that observed in 1928 (~2 m), the resulting Holocene rate would be large, about 0.9 mm/yr. This millimetric slip-rate is comparable to that observed on the well-developed normal faults in the Aegean [37]. Such a millimetric slip-rate on the Popovitza fault appears inconsistent with the long-term morphology.

The recent GPS investigations chow horizontal velocities of 2 +/-1 mm/year relative to the Eurasian plate in the Maritsa basin ([38] in according with onshore kinematics of central and eastern Mediterranean [39].

This suggests two possible interpretations to conciliate slip-rate and morphology. Either the morphology underestimates greatly the total throw and a millimetric slip-rate is possible over the long term or the total throw scales with the morphology and a millimetric slip rate cannot be extrapolated over a long timescale. In the former hypothesis the Popovitza fault, is under intense sedimentation in the footwall while erosion of the hanging wall erase the topography created by cumulative earthquakes. Sounding in the Maritsa basin should estimate the total offset on the Popovitza fault and help testing this hypothesis.

In the latter hypothesis, the Popovitza fault and the prominent Asenovgrad fault would interact to accommodate a millimetric slip rate. The two faults can be alternatively activated allowing for a more reasonable Holocene slip rate for the Popovitza fault. This kind of fault geometry has also been observed for the Grevena earthquake (M=6.6, 1995) that ruptured minor fault segments (topographic relief < 50 m), 10 km in front of a prominent Quaternary faults (topographic relief > 500 m and millimetric slip-rate, see Meyer *et al.* 1996) that were not activated during the event. Similarly, in the gulf of Corinth, the 5 m high Kaparelli fault scarp has been reactivated by the 1981 earthquake, in the hanging wall of the 400 m high escarpment of Livadostras fault that remained quiescent in 1981 [37].

This analysis combined with the paleosismologic investigations achieved by [27], suggest that the fault system activity between Balkan and Rhodope is not negligible. The 1928 coseismic deformation delineates a 20 km-wide graben, nested in a larger 40 km-wide graben between the Rhodope and the Balkan (Figure 1, 6). It is similar to a rift-in-rift structure as observed in the Corinth Golf, or along the oceanic rifts as the Asal rift in Djibouti. In that geometry, the inner faults and outer faults can be activated during the same period of time and alternate with inner faults and outer-faults earthquakes. With time, the activity migrates from the shoulder to the axis of the graben, and implies that the inner faults are younger than the outer faults. If the Balkan and the Asenovgrad fault control the large scale morphology of the Upper Thrace Lowland of Bulgaria the present day Maritsa river course is controlled by the Popovitza fault and probably its eastern prolongation along the Maritsa river, as illustrated with the vertical co-seismic deformation profile of Figure 6.

Acknowledgements

This work is initiated in the frame project of collaboration between the Bulgarian Academy of Sciences, INSU -CNRS and IPG Paris, France. We thank G. King for the fruitful discussions.

References:

1. Richter, C. F., 1958. Elementary seismology, Ed. W. H. Freeman, San Francisco, 768 p.
2. Ambraseys, N.N. & Jackson, J.A., 1998. Faulting associated with historical and recent earthquakes in the Eastern Mediterranean region, Geophys. J. Int., 133(2), 390–406.
3. Christoskov, L. & Grigorova, E., 1968. Energetic and space-time characteristics of the destructive earthquake in Bulgaria after 1900, Bull. Geophys. Inst., Bulg. Acad. Sci., 12, 79–107.
4. Karnik, V., 1969. Seismicity of the European Area, part 1, Ed. Academia, Prague.
5. Bonchev, S. & Bakalov, P., 1928. Les séismes du Sud de Bulgarie, Revue de Société géologique de Bulgarie, 1(2), 8- 21, Sofia.
6. Zelkov, Y., 1929. Report Department scientific, Agricultural Ministry, Sofia, 10(1-2), 3-6, (in Bulgarian).
7. Mihaillovic, J., 1928. Les grands tremblements de terre en Bulgarie en 1928, CRAS, Paris, 186, 1562–1563.
8. Mihailovic, J., 1928. Tremblements de terre de Bulgarie en 1928: Situation géologique des régions dévastées et dislocations diverses, CRAS, Paris, 186, 1741–1743.
9. DIPOZE, 1931, Direction Report for the mitigation of the 1928 Bulgarian earthquakes, Monograph, 421 p., Sofia.
10. Kirov, K., 1935. Study of the earthquakes of April 14 and April 18, 1928, Monograph, BAS, Sofia, 116 p.

11. Mirkov, M., 1932. Precision levelling measurements in the seismogenic zone of southern Bulgaria, Bull. Inst. Nat. Geogr., 34–39, Sofia.
12. Jankow, K., 1938. Niveauanderungen im Schuttergebiet der Erdbeben in Sudbulgarien am 14. und 18. April , Zeitschr. fur Geophys., Jahrgà. 14, Heft 1/ 2, 20–26.
13. Yankov, K., 1945. Changes in ground level produced by the earthquakes of April, 14 and April, 18 1928 in southern Bulgaria. In: Tremblements de Terre en Bulgarie, 29-31, 131-136, National Metheo Ins., Sofia.
14. Jackson, J. & McKenzie, D., 1983, The geometrical evolution of normal fault systems, Journal of Structural Geology, 5(5), 471–482.
15. Rangelov, B., Rizhikova, S. & Dimitrov, D., 1984. Plovdiv residual deformations of the 1928 earthquake and determination of the new parameters, Geologica Balcanica, 14(5), 67–72.
16. Dimitrov, D. & Ruegg, J-C., 1994. The 1928 Bulgarian earthquakes: fault geometry from geodetic data and modelling, Proc. 1st International Symposium on Deformations in Turkey, Istanbul, 921–932.
17. Jolivet, L., Brun, J.-P., Gauthier, P., Lallemant, S. & Patriat, M., 1994. 3D-kinematrics of extension in the Aegean region from the early Miocene to the present, insights from the ductile crust, Bull. Soc. Geol. France, 165, 195–209.
18. Burchfiel, B.C., Nakov, R., Tzankov, T. & Royden, L. 2000. Genozoic extension in Bulgaria and northern Greece: The northern part of the Aegen extensinal regime, Geol. Soc. London, Spec.Pub. 173, 325–352.
19. Armijo, R., Meyer, B., King, G.C.P., Rigo, A. & Papaanastassio, D., 1996, Quaternary evolution of the Corinth Rift and its implications for the evolution of Aegean, Geophys. J. Int., 126, 11–53.
20. Armijo, R, Meyer, B., Hubert, A. & Barka, A., 1999. Westwards Propagation on the North Anatolian Fault into the Northern Aegean: Timing and kinematics, Geology, 27, 267–270.
21. Mercier, J.L., Mouyaris, N., Simeakis, C., Roundoyanni, T. & Angelidhis, C., 1979. Intraplate tectonics: a quantitative study of the faults activated by the 1978 Thessaloniki earthquakes, Nature, 278, 45–48.
22. Soufleris, C., Jackson, J.A., King, G.C.P., Spencer, C.P. & Scholz, C.H., 1982. The 1978 earthquake sequence near Thessaloniki (Northern Greece), Geoph. J. R. astr. Soc., 68, 429–458.
23. Meyer, B., Armijo, R. & Dimitrov, D., 2002. Active faulting in SW Bulgaria: possible surface rupture of the 1904 Struma earthquakes, Geophys. J. Int. 148, 246–255.
24. UNESCO, 1974. Catalogue of Earthquakes, Survey of Seismicity of Balkan Region, Skopje, Part I, II, 600 p.
25. Mihailovic, J., 1933. La seismicite de la Bulgarie du Sud, UGGI Monography, serie B, Fasc. 3, 54 p. Beograd. 26. Kirov, K. & Grigorova, E., 1961. Seismicity in the Maritza valley, Bull. Geophys. Ins 2, BAS, Sofia, pp.5–55.
27. Vanneste, K., Radulov., A., De Martini, P., Nikolov, G., Petermans, T., Verbeek, K., Camelbeeck., T., Pantosti, D., Dimitrov, D. & Shanov, S., 2006. Paleoseismologic investigation of the fault rupture of the 14 April 1928 Chirpan earthquake (M 6.8), southern Bulgaria, Journal of Geophysical Research, 111(B01303), doi:10.1029/2005JB003814.
28. Rijikova, S., 1996. Earthquake catastrophes, Sofia, 192 p. (in Bulgarian).
29. Muir-Wood, R., & King, G.C.P., 1993. Hydrological signatures of earthquake strain, J.Geophys.Res. 98(B12), 22035-22060.
30. Christoskov, L., 1998. 70 years of Earthquakes in Chirpan – Plovdiv 1928, Symposium Geodynamic Investigations Related to the 1928 Earthquakes in Chirpan – Plovdiv, Sofia 09 October 1998, Bulg. Acad. Sci., 5–24.
31. Glavcheva, R., 1984. Characteristic of the destructive earthquake of April 18, 1928 M = 7.0) in Southern Bulgaria, Geophys. Journal, XVI(4), 38-44, BAS, Sofia.
32. Okada, Y., 1985. Surface deformation due to shear and tensile faults in a half-space, B.S.S.A.,75(4), 1135–1154.
33. Van Eck, T. & Stoyanov, T., 1996. Seismic hazard modelling for southern Bulgaria, Tectonophysics, 262, 77–100.
34. Lyon-Caen, H., Armijo, R., Drakopoulos, J., Baskoutas, J., Delibassis, N., Gaulon, R., Kouskouna, V.,Latoussaki, J., Makropoulos, K., Papadimitriou, P., Papanastassiou D. & Pedotti, G., 1988. The 1986 Kalamata (South Peloponnesus) earthquake: detailed study of a normal fault, evidences for east-west extension in the Helenic Arc. J. Geophys. Res., 93(B12), 14967–15000.
35. Armijo, R., H. Lyon-Caen and D. Papanastassiou, 1991, A possible normal-fault rupture for the 464 B.C. Sparta earthquake, Nature, 351, 123–125.
36. Meyer, B., Sébrier, M. & Dimitrov, D., 2006. Rare destructive earthquakes in Europe: The 1904 Bulgaria event case, Earth Planet. Sci. Lett., 10.1016/j.epsl.2006.11.011.
37. Benedetti, L., Finkel, R., King, G., Armijo, R., Papanastassiou, D., Ryerson, F., Flerit, F., Farber, D. &Stavrakakis, G., 2003. Motion on the Kaparelli fault (Greece) prior to the 1981 earthquake sequence determined from 36Cl cosmogenic dating, Terra Nova, 15, 118–124.
38. Kenyeres, A., T. Jambor, A. Caporali, B. Drosčak, B. Garayt, I. Georgiev, I. Jumare, J. Nagl, P. Pihlak, M. Ryczywolski, G. Stangl, 2013. Integration of the EPN and dense National permanent networks, Report of reference frame coordinator, EUREF 2013 Synposium, 29-31 May 2013, Budapest.
39. Pérouse E., N. Chamot-Rooke, A. Rabaute, P. Briole, F. Jouanne, I. Georgiev, D. Dimitrov 2012. Bridging onshore and offshore present-day kinematics of central and eastern Mediterranean: Implications for crustal dynamics and mantle flow, Geochemistry, Geophysics, Geosystems (G3), VOL. 13, 1525–2027.